International Journal of Research
Available at https://edupediapublications.org/journals

e-ISSN: 2348-6848
p-ISSN: 2348-795X
Volume 04 Issue 14
November 2017

An High Equipped Image Reconstruction Framework Based on Morphologic Regularization approach Using Bregman Iteration SR algorithm

Prashant B. Raule & Ravindra P. Shelkikar
(M.E. Scholar)[1] (Associate Professor)[2]

Electronics and Telecommunication Engineering Department[1,2]

[1,2]TPCT's College of Engineering, District- Osmanabad, (M.S.), India.

[1]raule.prashant@gmail.com [2]rpshelkikar@gmail.com

Abstract

Feature extractions are the novel techniques in image processing to store its unique characteristics. Morphological operators are the best for any image processing applications because it helps to preserve some characteristics from image. Although morphological operators is successful in solving the feature extraction but it too has some drawbacks. In this paper we model a non linear regularization method based on multi scale morphology for edge preserving super resolution (SR) image reconstruction. We formulate SR reconstruction problem from low resolution (LR) image as a deblurring and denoising and then solve the inverse problem using Bregman iterations. The proposed Method can be reduce inherent noise generated during low-resolution image formation as well as during SR image estimation efficiently. Using MATLAB simulation results we showed the effectiveness of the proposed method and reconstruction method for SR image.

I. INRODUCTION

The basic goal is to develop an algorithm to enhance the spatial resolution of images captured by an image sensor with a fixed resolution. This process is called the super resolution (SR) method and it has remained an active research topic for the last two decades. Super-resolution (SR) technique reconstructs a higher-resolution image or sequence from the observed LR images. As SR has been developed for more than three decades, both multi-frame and single-frame SR have significant applications in our daily life.SR algorithms may vary depending on whether only a single low-resolution (LR) image is available (single frame SR) or multiple LR images are available (multi frame SR).

SR image reconstruction algorithms work either:
1) In the frequency domain or
2) In the spatial domain.

This paper focus only on spatial domain approach for multi frame SR image reconstruction. This paper is based on the regularization framework, where the HR image is estimated based on some prior knowledge about the image (e.g., degree of smoothness) in the form of regularization.

Bayesian maximum a posteriori (MAP) estimation based methods use prior information in the form of a prior probability density on the HR image and provides a rigorous theoretical framework. MAP based joint

International Journal of Research
Available at https://edupediapublications.org/journals
e-ISSN: 2348-6848
p-ISSN: 2348-795X
Volume 04 Issue 14
November 2017

formulation is proposed that judiciously combine motion estimation, segmentation, and SR together. The probability based MAP approach is equivalent to the concept of regularization. he first successful edge preserving regularization method for denoising and deblurring is the total variance (TV) (L1 norm) method. Another interesting algorithm, proposed by Farsiu et al., employs bilateral total variation (BTV) regularization.

SR is a technique which reconstructs a higher-resolution image or sequence from the observed LR images. Technically, SR can be

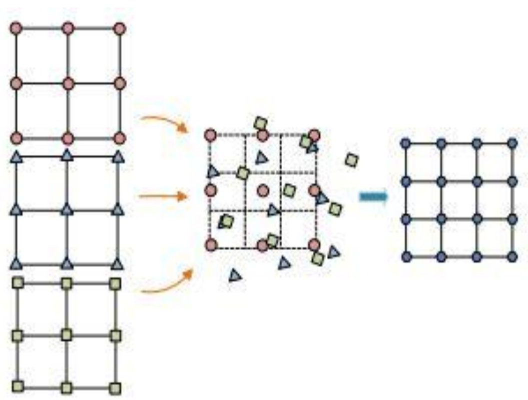

Fig. 1. The concept of multi-frame super-resolution. The grids on the left side represent the LR images of the same scene with sub-pixel alignment, thus the HR image (the grid on the right side) can be acquired by fusing the complementary information with SR methods.

A new regularization method based on multi scale morphologic filters is proposed, which are nonlinear in nature. Morphological operators and filters are well-known tools that can extract structures from images. Since proposed morphologic regularization term uses non differentiable max and min operators, developed an algorithm based on Bregman iterations and the forward backward operator splitting using sub gradients. The results produced by the proposed regularization are less affected by aforementioned noise evolved during the iterative process.

II. PROBLEM FORMULATION

The observed images of a scene are usually degraded by blurring due to atmospheric turbulence and inappropriate camera settings. The LR images are further degraded because of down sampling by a factor determined by the intrinsic camera parameters. The relationship between the LR images and the HR image can be formulated as

$$Y_k = DF_k H_k X + e_k, \quad \forall k = 1, 2, \ldots, K \qquad (1)$$

where Y_k , X, and ek represent lexicographically ordered column vectors of the kth LR image of size M, HR image of size N and additive noise, respectively. F_K is a geometric warp matrix and HK is the blurring matrix of size N×N incorporating camera lens/CCD blurring as well as atmospheric blurring. D is the down sampling matrix of size M × N and k is the index of the LR images. Assuming that the LR images are taken under the same environmental condition and using same sensor, H_K becomes the same for all k and may be denoted simply by H. the LR images are related to the HR image as

$$Y_k = DF_k HX + e_k, \quad \forall k = 1, 2, \ldots, K \qquad (2)$$

Since under assumption, D and H are the same for all LR images, avoid down sampling and then up sampling at each iteration of iterative reconstruction algorithm by merging the up sampled and shifted-back LR images Y_k together. After applying up sampling and reverse shifting, Y_k will be aligned with HR image X. Suppose Y_k denotes the up sampled and reverse-shifted kth LR image obtained through reverse effect of DFK of (2). That means Y_k = F-1DTYK,

International Journal of Research
Available at https://edupediapublications.org/journals
e-ISSN: 2348-6848
p-ISSN: 2348-795X
Volume 04 Issue 14
November 2017

where DT is the up sampling operator matrix of size N × M and is an N × N matrix that shifts back (reverse effect of F_K) the image. The equation from (2), (3), (4) as,

$$\underline{Y} = RHX + \underline{e} \qquad (3)$$

$$\hat{X} = arg \min_X \left[\left\| RHX - \underline{Y} \right\|_2^2 \right] \qquad (4)$$

Regularization has used in conjunction with iterative methods for the restoration of noisy degraded images in order to solve an ill-posed problem and prevent over-fitting. Then the SR image reconstruction can simply be formulated as

$$\hat{X} = arg \min_X \left[\Upsilon(X) : \left\| RHX - \underline{Y} \right\|_2^2 < \eta \right] \qquad (5)$$

Where η is a scalar constant depending on the noise variance in the LR images

III. Proposed Work

A. Morphologic Regularization

Let B be a disk of unit size with origin at its center and SB be a disk structuring element (SE) of size s. Then the morphological dilation DS (X) of an image X of size M X N at scale S is defined as

$$D_s(X) = \begin{pmatrix} max_{r\in(sB)_{(1)}}\{x_r\} \\ max_{r\in(sB)_{(2)}}\{x_r\} \\ \ddots \\ max_{r\in(sB)_{(mn)}}\{x_r\} \end{pmatrix} \qquad (6)$$

Where (SB)(I) is a set of pixels covered under SE SB translated to the I -th pixel XI . Similarly, the morphological erosion ES (X) at scale S is defined as

$$E_s(X) = \begin{pmatrix} \min_{r\in(sB)(1)}\{x_r\} \\ \min_{r\in(sB)(2)}\{x_r\} \\ \cdot \\ \cdot \\ \cdot \\ \min_{r\in(sB)(mn)}\{x_r\} \end{pmatrix} \qquad (7)$$

Morphological opening OS (X) and closing CS (X) by SE SB are defined as follows:

$$O_s(X) = D_s\big(E_s(X)\big) \qquad (8)$$

$$C_s(X) = E_s\big(D_s(X)\big) \qquad (9)$$

In multi scale morphological image analysis, the difference between the s^{th} scale closing and opening extracts noise particles and image artifacts in scale S and may be used for denoising purposes.

B. Subgradient Methods and Bregman Iteration

Bregman iteration is used in the field of computer vision for finding the optimal value of energy functions in the form of a constrained convex functional. In constrained and unconstrained problems, the “fixed point continuation” (FPC) method is used to solve the unconstrained problem by performing gradient descent steps iteratively. The linearized Bregman algorithm is derived by combining the FPC and Bregman iteration to solve the constrained problem in a more efficient way. An algorithm is developed on Bregman iteration and the proposed morphologic regularization for the SR image reconstruction problem.

C. Bregman Iteration

The proposed penalized splitting approach and corresponds to an algorithm whose structure is characterized by two-level iteration. There is an outer loop, which progressively diminishes the penalization parameter λ in order to obtain the convergence to the global minimum, and an inner loop, which iteratively, using the two-step approach, minimizes the penalization function for the given value of λ. The general scheme of the bound constrained algorithm is the following.

Initialize $\mathrm{Y}^{(0)} = \mathrm{n} = 0, \underline{Y}, \mathrm{X}^{(0)} = \mathrm{FillUnknown}(\underline{\mathrm{Y}})$;

While$\left(\left\|RHX^{(n)} - \underline{\mathrm{Y}}\right\|_2^2 > \eta\right)$

$$\begin{cases} U^{(n+1)} = \mathrm{X}^{(n)} - \gamma H^T R^T (\mathrm{RHX}^{(n)} - \mathrm{Y}^{(n)}) \\ X^{(n+1)} = U^{(n+1)} - \mu' \left|\frac{\delta \mathrm{Y(X)}}{\delta(\mathrm{X})}\right|_{\mathrm{X}^{(n)}} \\ Y^{(n+1)} = Y^{(n)} + \left(\underline{Y} - RHX^{(n+1)}\right) \\ n = n+1 \end{cases} \quad (10)$$

Here we derive the sub gradients of the dilated and eroded image with respect to its pixel values. Let us denote the sub gradient of a dilated image Ds(X)

$$\frac{\delta D_{s,j}}{\delta x_i} = \begin{cases} 1, & \text{if } x_i = \max\limits_{r\epsilon(sB)_{(j)}} \{x_r\} \text{ and} \\ & \forall t \in (sB)_{(j)}, t \neq i, x_t < x_i \\ 0, & \text{if } x_i < \max\limits_{r\epsilon(sB)_{(j)}} \{x_r\} \\ \epsilon[0,1], & \text{elsewhere} \end{cases} \quad (11)$$

Similarly, the sub gradient of an eroded image Es(X) can be written as follows. We choose the sub gradient equal to 1 out of the range [0, 1]. Then the sub gradients become

$$\frac{\delta D_{s,j}}{\delta x_i} = \begin{cases} 1, & \text{if } x_i = \max\limits_{r\epsilon(sB)_{(j)}} \{x_r\} \\ 0, & \text{if } x_i < \max\limits_{r\epsilon(sB)_{(j)}} \{x_r\} \end{cases} \quad (12)$$

$$\frac{\delta E_{s,j}}{\delta x_i} = \begin{cases} 1, & \text{if } x_i = \max\limits_{r\epsilon(sB)_{(j)}} \{x_r\} \\ 0, & \text{if } x_i < \max\limits_{r\epsilon(sB)_{(j)}} \{x_r\} \end{cases} \quad (13)$$

Since an analogous chain rule holds for the sub gradients, we can write down the sub gradients of the regularization function

$$\frac{\delta \mathrm{Y(X)}}{\delta(\mathrm{X})} := \frac{\delta}{\delta \mathrm{X}} \sum_{s=1}^{K} \alpha^s 1^t [C_s(X) - O_s(X)]$$

$$= \sum_{s=1}^{K} \alpha^s \left[\frac{\delta C_s(\mathrm{X})}{\delta \mathrm{X}} - \frac{\delta O_s(\mathrm{X})}{\delta \mathrm{X}}\right] 1$$

$$= \sum_{s=1}^{K} \alpha^s \left[\frac{\delta}{\delta \mathrm{X}} E_s(D_s(X)) - \frac{\delta}{\delta \mathrm{X}} D_s(E_s(X))\right] 1$$

$$= \sum_{s=1}^{K} \alpha^s \left[\frac{\delta}{\delta D_s(X)} E_s(D_s(X)) \frac{\delta}{\delta \mathrm{X}} D_s(X)\right] - \left[\frac{\delta}{\delta E_s(X)} D_s(E_s(X)) \frac{\delta}{\delta \mathrm{X}} E_s(X)\right] 1 \quad (14)$$

The respective erosion and dilution functions are illustrated as follows

$$q_i^{E_{s,j}} := \frac{\delta E_{s,j}}{\delta d_{s,i}} = \begin{cases} 1, & \text{if } d_{s,i} = \max\limits_{r\epsilon(sB)_{(j)}} \{d_{s,i}\} \\ 0, & \text{if } d_{s,i} < \max\limits_{r\epsilon(sB)_{(j)}} \{d_{s,i}\} \end{cases} \quad (15)$$

$$q_i^{Ds_{s,j}} := \frac{\delta D_{s,j}}{\delta e_{s,i}} = \begin{cases} 1, & \text{if } e_{s,i} = \max\limits_{r\epsilon(sB)_{(j)}} \{e_{s,i}\} \\ 0, & \text{if } e_{s,i} < \max\limits_{r\epsilon(sB)_{(j)}} \{e_{s,i}\} \end{cases} \quad (16)$$

IV. SIMULATION RESULTS

A. RESULTS FOR SR1

International Journal of Research
Available at https://edupediapublications.org/journals

e-ISSN: 2348-6848
p-ISSN: 2348-795X
Volume 04 Issue 14
November 2017

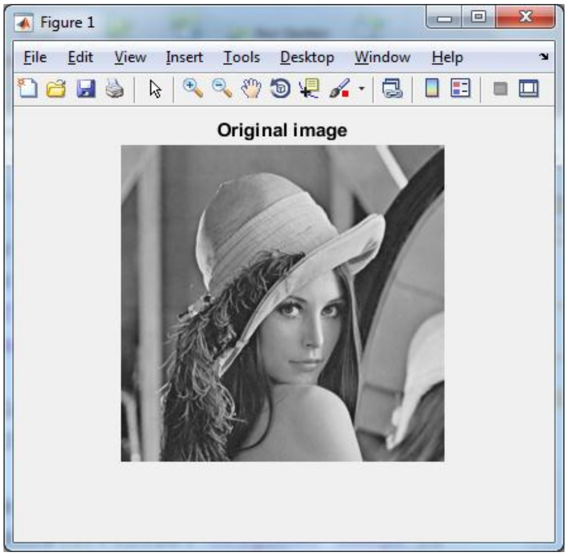

Figure 2 Comparison of reconstruction result of the chart image for misestimated motion model and erroneous Gaussian blur parameter. SR image reconstruction using (a) Grd +BTV

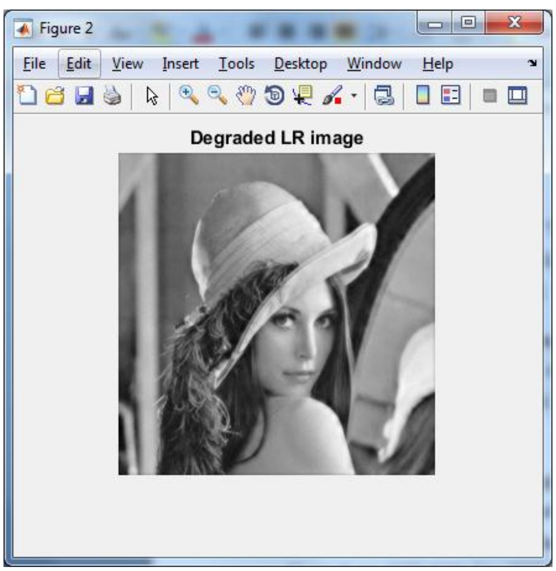

Figure 3 Comparison of reconstruction result of the chart image for misestimated motion model and erroneous Gaussian blur parameter. SR image reconstruction using (b) Breg+BTV

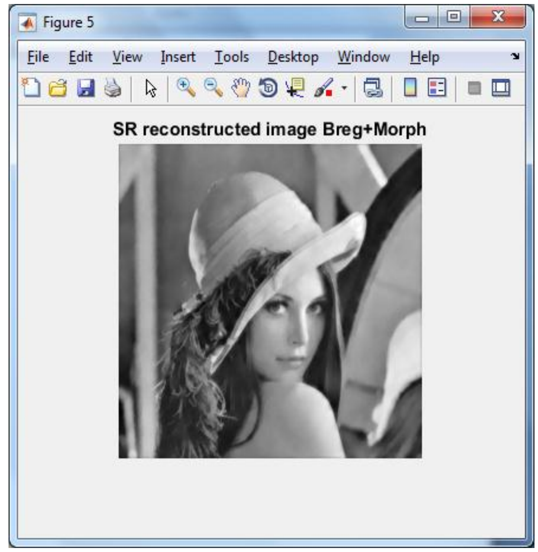

Figure 4 Comparison of reconstruction result of the chart image for misestimated motion model and erroneous Gaussian blur parameter. SR image reconstruction using (c) Breg +Morph (proposed method)

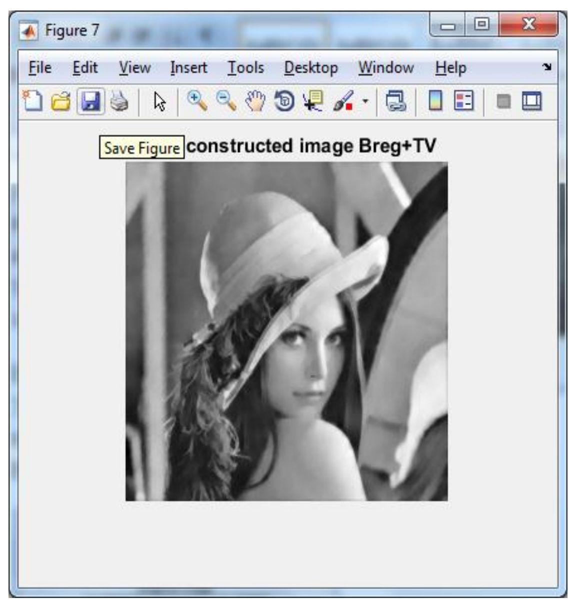

Figure 5 Comparison of reconstruction result of the chart image for misestimated motion model and erroneous

Gaussian blur parameter. SR image reconstruction using (c) Breg +TV .

B. RESULTS FOR SR2

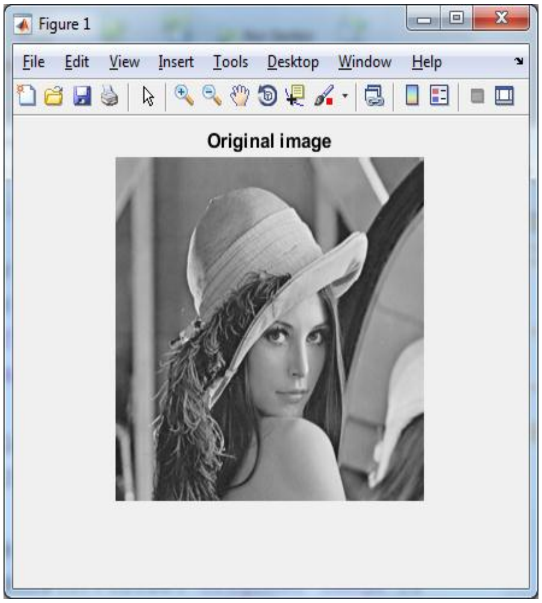

Figure 6 Results of the various SR image reconstruction methods with a small amount of noise (σ=2). (a) Original HR image of a chart.

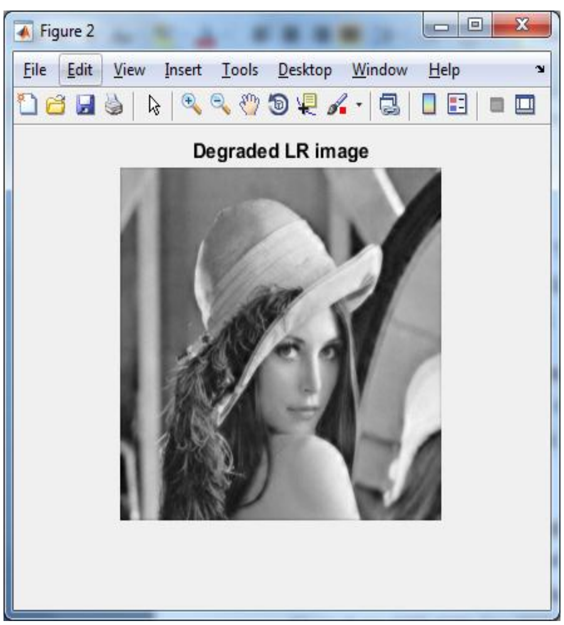

Figure 7 Results of the various SR image reconstruction methods with a small amount of noise (σ=2). (b) One of the generated LR images.

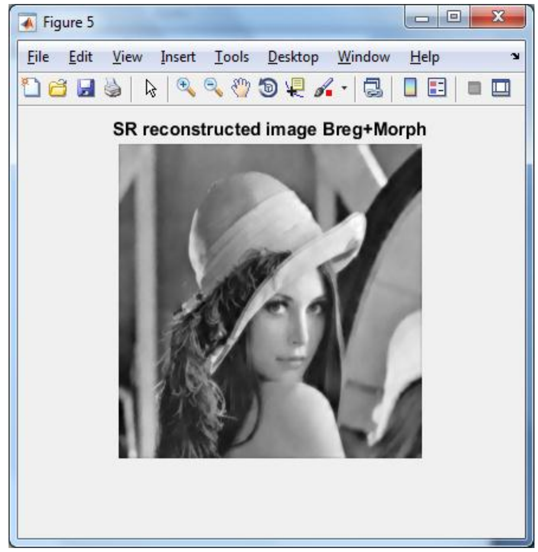

Figure 8 Results of the various SR image reconstruction methods with a small amount of noise (σ=2). (c) Up sampled and merged 10 LR images.

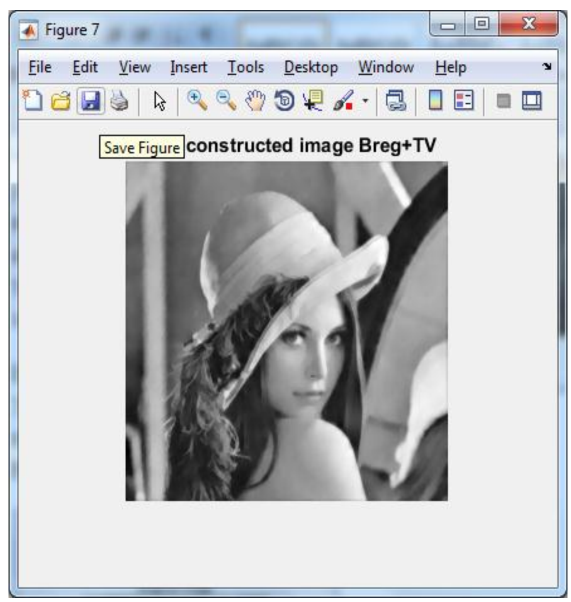

Figure 9 Results of the various SR image reconstruction methods with a small amount of noise (σ=2). SR

e-ISSN: 2348-6848
p-ISSN: 2348-795X
Volume 04 Issue 14
November 2017

reconstructed image using the gradient descent method with TV,BTV, and LABTV regularization, respectively.

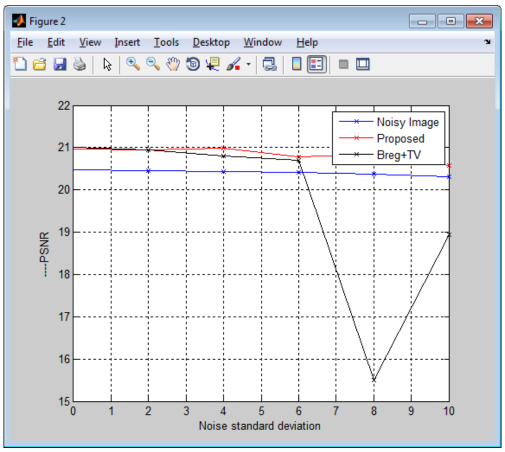

Figure 10 Analysis of the performance of SR image reconstruction algorithms applied on different gray images and then average quantitative measures are plotted. (a) PSNR and SSIM of SR algorithms for noisy LR images with additive Gaussian noise.

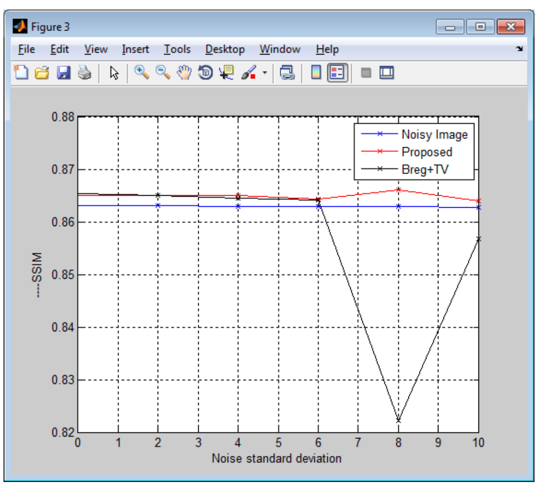

Figure 11 Analysis of the performance of SR image reconstruction algorithms applied on different gray images and then average quantitative measures are plotted. (b) PSNR and SSIM for different amount of misrediction in the blurring parameter.

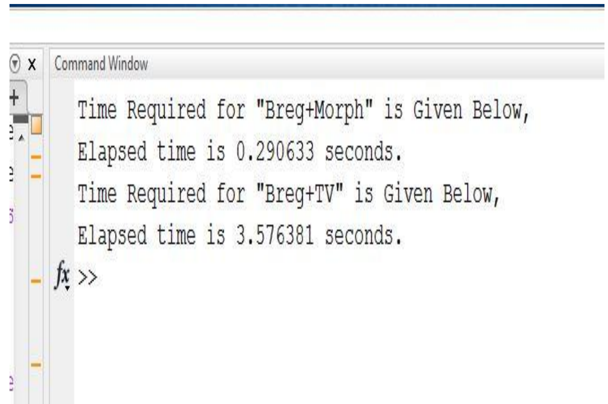

Table 1: Time required to execute the existing system(Breg+TV) and proposed work(Breg+Morph)

We studied theoretically that proposed work require less time for execution compared to state of art existing techniques.

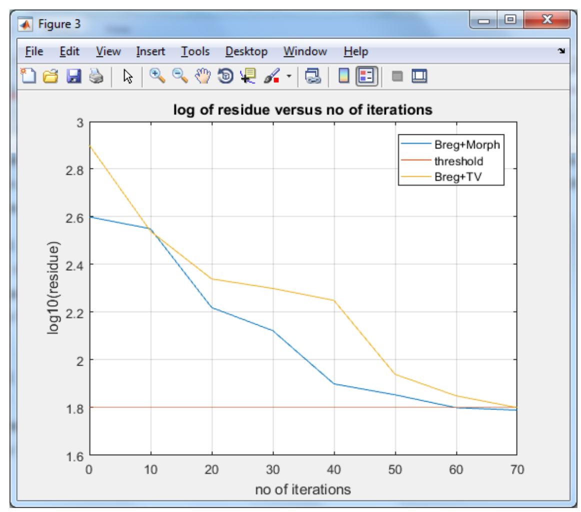

Figure 12 log of residue versus no of iterations plot

Here, we plotted log of residue versus no of iterations plot, which will give better performance of proposed work compared with state of art existing technique “Breg+TV”.

International Journal of Research
Available at https://edupediapublications.org/journals

e-ISSN: 2348-6848
p-ISSN: 2348-795X
Volume 04 Issue 14
November 2017

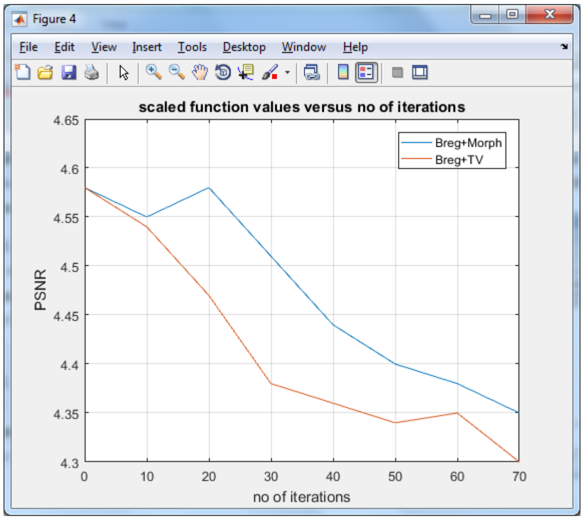

Figure 13 scaled function values versus no. of iterations.

These two plots, i.e., Fig.11 and 12, together show the reconstruction qualities of different methods with number of iterations.

Table 2: Comparative analysis of Existing (Breg+TV) and Proposed (Breg+Morph) Method

Different Images	Breg+ TV		Proposed Method	
	PSNR	SSIM	PSNR	SSIM
	30.4438	0.9940	35.6078	0.9948
	29.0320	0.9343	33.0751	0.9315
	27.2429	0.9735	32.1092	0.9730
	26.3673	0.9758	31.1846	0.9739
	28.2611	0.9921	34.1718	0.9934
	26.7441	0.8985	31.8901	0.8966
	27.6456	0.9943	33.0662	0.9938
	28.1086	0.9769	33.1717	0.9769
	23.6189	0.9780	28.1661	0.9786
	26.2741	0.9915	31.1790	0.9916

➢ **Applications**

1. Regular video information enhancement
2. Surveillance
3. Medical diagnosis
4. Earth-observation remote sensing
5. Astronomical observation
6. Biometric information identification

V. Conclusion

This paper presented an edge-preserving SR image reconstruction problem as a deblurring problem with a new robust morphologic regularization method. Then put forward two major contributions. First, proposed a morphologic regularization function based on multi scale opening and closing, which could remove noise efficiently while preserving edge information. Next, employed Bregman iteration method to solve the inverse problem for SR reconstruction with the proposed morphologic regularization. Compare to previous algorithms proposed algorithm gives better results of quality parameters.Matlab simulations also shows that the proposed work is more efficient compared to all other existing techniques. For quality assessment we are going to use two parameters as PSNR and SSIM.It is known that multi scale morphological filtering can reduce noise efficiently, so a successfully regularization method is used based on multi scale morphology. The experimental results show that it works quite well, in fact better than existing methods. Nonlinearity of the regularization function is handled in a linear fashion during optimization by means of the sub gradient and proximal map concept. The morphologic

e-ISSN: 2348-6848
p-ISSN: 2348-795X
Volume 04 Issue 14
November 2017

regularization method proposed here was tested only on SR reconstruction problem; this method is extended by computing Blocking effect, Homogeneity and ISNR.

REFERENCES

[1] S. Lertrattanapanich and N. K. Bose, "High resolution image formation from low resolution frames using Delaunay triangulation," IEEE Trans. Image Process., vol. 11, no. 12, pp. 1427–1441, Dec. 2002.

[2] A. J. Patti and Y. Altunbasak, "Artifact reduction for set theoretic super resolution image reconstruction with edge adaptive constraints and higher-order interpolants," IEEE Trans. Image Process., vol. 10, no. 1, pp. 179–186, Jan. 2001.

[3] M. Elad and A. Feuer, "Restoration of a single super resolution image from several blurred, noisy and under sampled measured images," IEEE Trans. Image Process., vol. 6, no. 12, pp. 1646–1658, Dec. 1997.

[4] H. Shen, L. Zhang, B. Huang, and P. Li, "A MAP approach for joint motion estimation segmentation and super resolution," IEEE Trans. Image Process., vol. 16, no. 2, pp. 479–490, Feb. 2007.

[5] W. T. Freeman and T. R. Jones, "Example-based super resolution," IEEE Comput. Graphics Appl., vol. 22, no. 2, pp. 56–65, Mar. 2002.

[6] J. Yang, J. Wright, T. S. Huang, and Y. Ma, "Image super-resolution via sparse representation," IEEE Trans. Image Process., vol. 19, no. 11, pp.2861–2873, Nov. 2010.

[7] K. I. Kim and Y. Kwon, "Single-image super resolution using sparse regression and natural image prior," IEEE Trans. Pattern Anal. Mach. Intell., vol. 32, no. 6, pp. 1127–1133, Jun. 2010.

[8] W. Dong, L. Zhang, G. Shi, and X. Wu, "Image deblurring and super resolution by adaptive sparse domain selection and adaptive regularization," IEEE Trans. Image Process., vol. 20, no. 7, pp. 533–549, Jul. 2011.

[9] M. Protter, M. Elad, H. Takeda, and P. Milanfar, "Generalizing the nonlocal-means to super-resolution reconstruction," IEEE Trans. Image Process., vol. 18, no. 1, pp. 36–51, Jan. 2009.